PHILOSOPHICAL TRANSACTIONS OF THE ROYAL SOCIETY B BIOLOGICAL SCIENCES

Amperometric Enzyme Electrodes [and Discussion]

W. J. Albery, P. N. Bartlett, A. E. G. Cass, R. Eisenthal, I. J. Higgins and M. Aizawa

Phil. Trans. R. Soc. Lond. B 1987 **316**, 107-119
doi: 10.1098/rstb.1987.0021

Phil. Trans. R. Soc. Lond. B **316**, 107–119 (1987) [107]
Printed in Great Britain

Amperometric enzyme electrodes

By W. J. Albery, F.R.S., P. N. Bartlett† and A. E. G. Cass
Department of Chemistry and Centre for Biotechnology, Imperial College of Science and Technology, London SW7 2AY, U.K.

Three different types of amperometric enzyme electrode are described. The first type uses a conducting organic-salt electrode to oxidize NADH. Results for sensors for ethanol and for bile acids are presented. In the second type of sensor, flavoenzymes are directly oxidized on the surface of the conducting organic-salt electrode. Results for five different enzymes are described. The mechanism of the enzyme oxidation is discussed and the reaction is shown to take place by heterogeneous redox catalysis and not by homogeneous mediation. The enzymes are strongly adsorbed on the electrode; microelectrodes for *in vivo* studies can be constructed without a membrane. Results for *in vivo* studies of changing glucose levels in the brain of a freely moving rat are presented. The third type of sensor is designed to measure low levels of toxic gases such as H_2S and HCN. This is done by monitoring the inhibition by the toxic gas of the activity of the respiratory enzyme cytochrome oxidase.

Introduction

In this paper we describe the development of three different types of amperometric enzyme electrode. Over 250 enzymes use the unbiquitous cofactor β-nicotinamide adenine dinucleotide (NAD^+) to oxidize a substrate SH_2 to S, the cofactor being reduced to NADH. Following the work of Kulys and co-workers (Kulys *et al.* 1980, 1982; Kulys & Samalius 1983), we showed that conducting organic salts are efficient electrode materials for the rapid electrochemical oxidation of NADH (Albery & Bartlett 1984). Hence the first type of sensor to be described has the following reaction scheme:

$$NAD^+ + SH_2 \xrightarrow{\text{enzyme}} NADH + S + H^+$$

$$NADH \xrightarrow{NMP^+TCNQ^-\text{electrode}} NAD^+ + H^+ + 2e^-.$$

The structures of NMP^+ and TCNQ are shown in scheme 1.

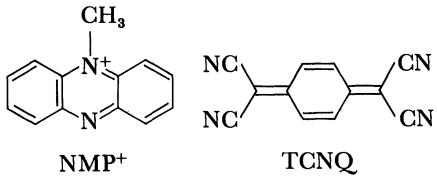

NMP^+ TCNQ

Scheme 1

We have also found that the active sites of a number of flavo-enzymes can be oxidized on the surface of electrodes made of conducting organic salts (Albery *et al.* 1985, 1986). This has led to the development of the second type of sensor described in this paper, where the substrate

† Present address: Department of Chemistry, University of Warwick, Coventry CV4 7AL, U.K.

is oxidized by the enzyme and the active site of the enzyme (FAD–$FADH_2$) is then regenerated electrochemically:

$$SH_2 + FAD \rightarrow S + FADH_2;$$

$$FADH_2 \xrightarrow{TTF^+TCNQ^-\text{electrode}} FAD + 2H^+ + 2e^-$$

The structure of TTF is shown in scheme 2. This is the simplest possible reaction scheme for an enzyme electrode. We have classified this type of electrode as a third-generation electrode

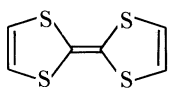

SCHEME 2

to distinguish it from a first-generation electrode, where the natural reactant, oxygen, oxidizes the active site, and a second-generation electrode where a mediator (such as ferrecinium) is used (Hill, this symposium). In this paper, we will discuss the mechanism by which the active site is oxidized on the electrode surface and we will also describe the application of this type of sensor to the direct *in vivo* monitoring of glucose levels in the brain of a freely moving rat (Boutelle *et al.* 1986).

The third type of sensor is designed to measure low levels of toxic gases such as H_2S or HCN. The concentrations of a few parts per million (by volume) are so low that the current from the flux of gas molecules is too small to be measured. To overcome this problem we have constructed a chemical canary, in which the respiratory enzyme cytochrome oxidase reduces oxygen and the rate of this reaction is monitored as a current. When a molecule of the enzyme is 'killed' by a toxic gas molecule, the current falls. The greater sensitivity is achieved because each toxic gas molecule 'kills' a molecule of the enzymic catalyst, which has a high turnover, and hence the effect on the current is much greater than if one merely carried out a two-electron reduction or oxidation of the offending gas.

NADH ELECTRODES

We have shown (Albery & Bartlett 1984) that NADH can be oxidized on an NMP^+TCNQ^- electrode. The electrode is stable between -0.1 and $+0.3$ V (with respect to a saturated calomel electrode, SCE). Throughout this range the rate of oxidation of NADH does not vary significantly with potential. Rotating disc studies give linear Koutecky–Levich plots (Koutecky & Levich 1956) showing that mass transfer to the disc electrode is partially rate limiting. These plots are shown in figure 1. The intercepts of these plots, which correspond to the rate at infinite rotation speed, vary linearly with $[NADH]^{-1}$. This plot is equivalent to a Lineweaver–Burke plot in enzyme kinetics, to find the Michaelis–Menten parameters, or to a plot for a Langmuir isotherm. The simplest explanation is that the NADH is adsorbed fairly strongly onto the electrode surface with an association constant of about 1 mM^{-1}. This adsorption results in a moderately rapid electrochemical rate constant of 10^{-3} cm s^{-1}.

In table 1 we collect together a number of possible analytes and enzymes that conform to scheme 1 above. In our work we have developed a sensor for ethanol, based on alcohol dehydrogenase. Typical results are displayed in figure 2. Application of kinetic analysis with

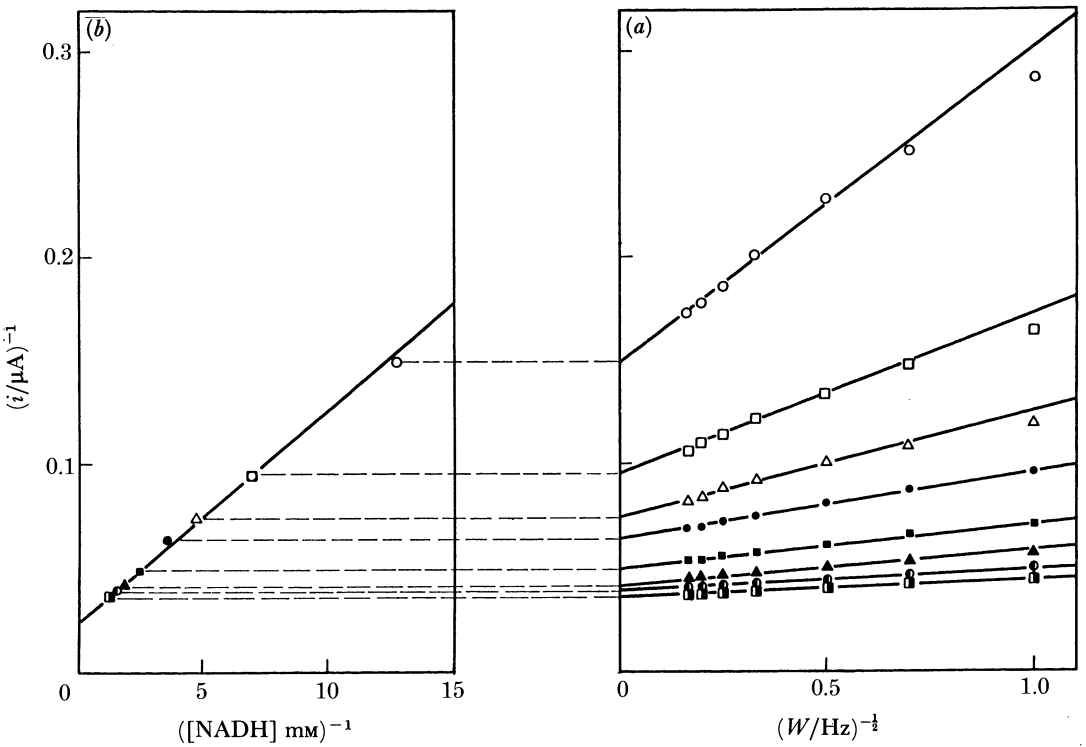

FIGURE 1. (*a*) Koutecky–Levich plots of the current, i, against the rotation speed, W, for the oxidation of NADH on a rotating pellet electrode (0.52 cm², $E = 0.25$ V w.r.t. SCE, 0.1 M LiCl, Tris buffer pH 8.0). The intercepts of the plots in (*a*) are plotted against $[NADH]^{-1}$ in (*b*).

TABLE 1. NAD^+–NADH ENZYME SYSTEMS

analyte	enzyme	application
alcohol	alcohol dehydrogenase	fermentation
lactate	lactate dehydrogenase	dairy industry
malate	malate dehydrogenase	fermentation
glutamate	glutamate dehydrogenase	fermentation food industry
glucose	glucose dehydrogenase	fermentation clinical
glycerol	glycerol dehydrogenase	fermentation
bile acids	11_B hydroxysteroid dehydrogenase	clinical
nitrate	nitrate reductase	agriculture water industry
oestradiol	oestradiol 17_B dehydrogenase	agriculture food industry clinical
amino acids	amino acid dehydrogenase	fermentation clinical food industry

a 'rho plot' (Albery & Bartlett 1985) shows that the rate-limiting processes controlling the current are the enzyme kinetics, and the value of the Michaelis constant of the enzyme electrode of 10 mM is in reasonable agreement with published values (Barman 1969; Burstein *et al.* 1981).

In collaboration with Professor R. H. Dowling and Dr G. Murphy of Guys Hospital, London, we are using the enzyme 3-hydroxysteroid dehydrogenase to develop a sensor for the

measurement of bile acids. The enzyme oxidizes the 3-hydroxy group to a carbonyl group. Calibration plots for a number of bile acids are displayed in figure 3. The sensor is so simple and cheap that we can look forward to an instant, direct-reading assay being carried out in the ward, as opposed to samples being taken to the hospital laboratory for a fairly cumbersome analytical procedure.

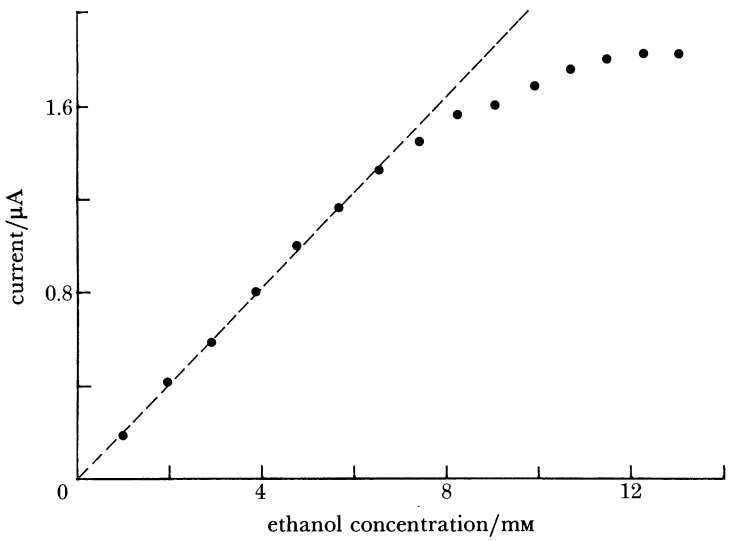

FIGURE 2. Typical results for the current from the ethanol electrode as a function of the concentration of ethanol.

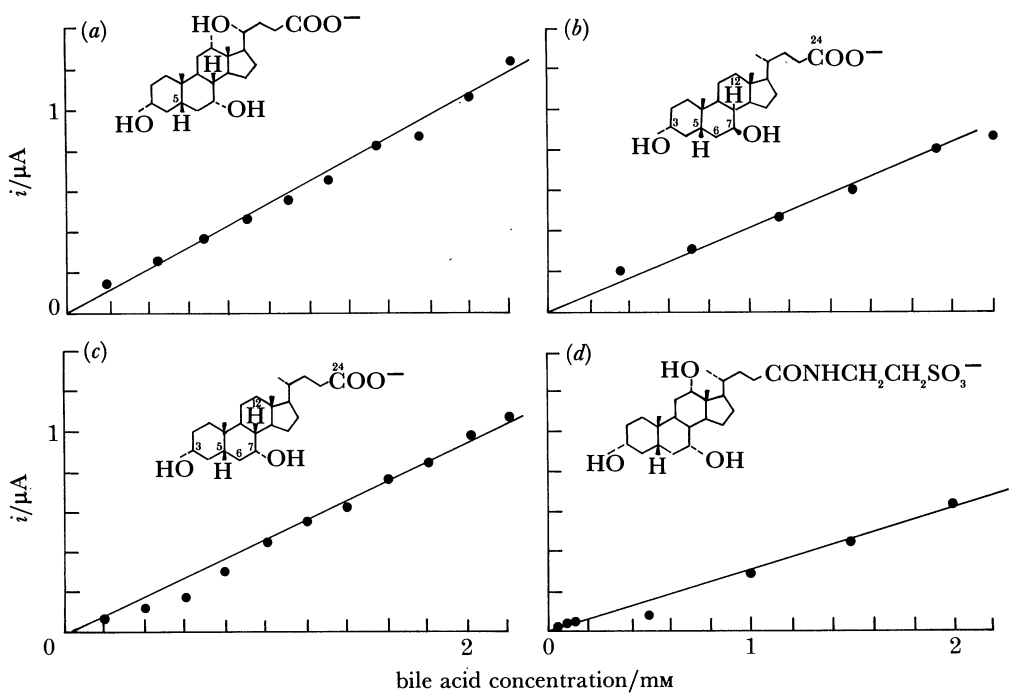

FIGURE 3. Results for the current from the bile-acid electrode for four different bile acids: (*a*), cholic acid; (*b*), ursodeoxycholic acid; (*c*), chenodeoxycholic acid; (*d*), taurocholic acid.

Flavo-enzyme electrodes

Next we turn to those systems (scheme 2 above) where we oxidize the enzyme itself on the electrode surface (Albery *et al.* 1985, 1986). In figure 4 and table 2 we present results for some of the systems we have studied. The kinetic anlaysis based on the rho plot shows that, for these systems, the rate limiting processes are diffusion of the substrate through the dialysis membrane and the oxidation of the enzyme's active site on the electrode. The only exception is the choline

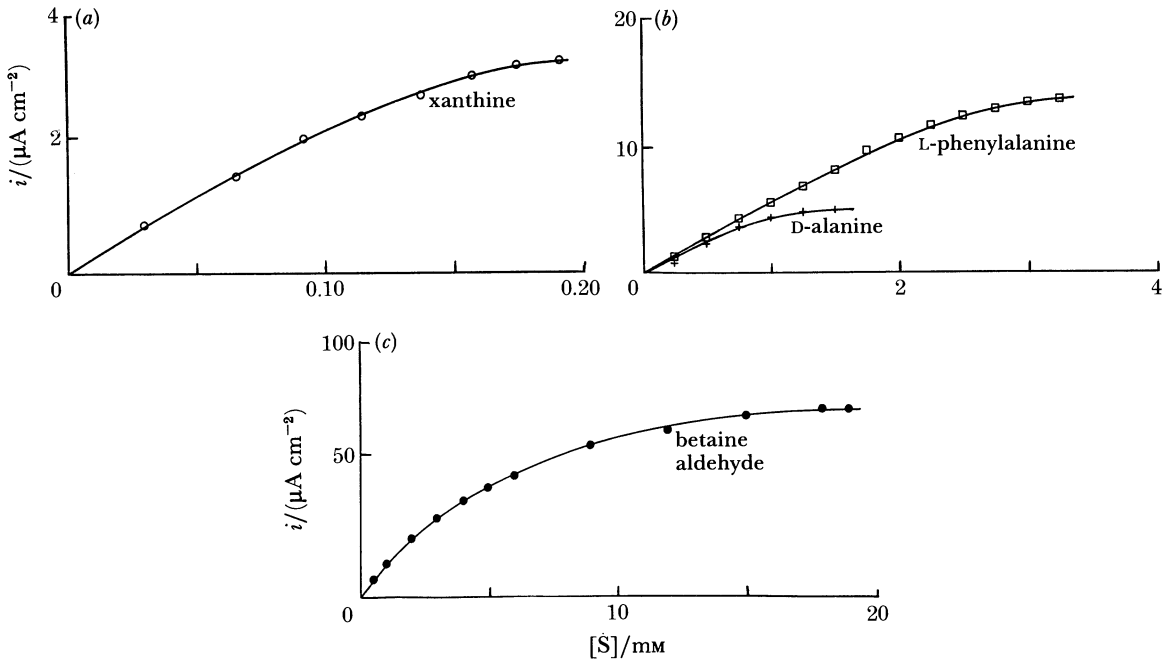

Figure 4. Typical results for four different substrates where the flavo-enzymes (xanthine oxidase, D- and L-amino acid oxidase and choline oxidase) are oxidized directly on a $TTF^{+}TCNQ^{-}$ electrode.

Table 2. Values of electrochemical rate constants for five enzyme–substrate systems

enzyme	substrate	$k'/(cm\ s^{-1})$
glucose oxidase	glucose	9×10^{-2}
D-amino acid oxidase	D-alanine	2×10^{-4}
L-amino acid oxidase	L-phenylalanine	5×10^{-2}
choline oxidase	betaine aldehyde	3×10^{-3}
xanthine oxidase	xanthine	4×10^{-4}

oxidase–betaine aldehyde combination where the unsaturated enzyme kinetics and the substrate transport are both partially rate-limiting. The electrochemical rate constants in table 2 are all moderately rapid and show that the conducting-salt electrode is a good electrocatalyst for the oxidation of the enzyme. Furthermore, these systems show excellent stability: a glucose electrode was run continuously for 28 days, and at the end of that period the electrode kinetics showed no loss of activity, although the transport of substrate through the membrane was some 10% slower (Albery *et al.* 1986*a*).

We have also found that these electrodes can be operated without any membrane at all. The

electrode is simply dipped into the enzyme solution and the enzyme is adsorbed so irreversibly onto the electrode that it cannot be washed off. The adsorbed enzyme is active and the enzyme electrode can be exposed directly to the substrate. As discussed below, this feature of the system is exploited in making microelectrodes for *in vivo* studies.

Electrode mechanism

There has been some controversy as to why these electrodes are so efficient. Kulys (Cenas & Kulys 1981) considers that the oxidation of the enzyme takes place by homogeneous reaction of the active site with dissolved components of the organic-salt electrode. Such a scheme is similar to the second-generation electrodes described by Hill (this symposium). For such a mechanism the flux, j/(mol cm^{-2} s^{-1}) is given by

$$j = k[\mathrm{E}][\mathrm{M}]\, X_{\mathrm{k}}, \tag{1}$$

where k is the second-order rate constant for the homogeneous reaction of E and M, [E] is the concentration of reduced enzyme,[M] is the surface concentration of dissolved mediator and X_{k} is the thickness of the reaction layer. This thickness describes how far M will diffuse before being destroyed be E:

$$X_{\mathrm{k}} = \sqrt{(D/k[\mathrm{E}])}. \tag{2}$$

Substitution of (2) in (1) gives

$$j = \sqrt{(Dk[\mathrm{E}])}\,[\mathrm{M}]. \tag{3}$$

Stopped-flow results (Cenas & Kulys 1981) show that $k < 10^{6}$ M^{-1} s^{-1}. Hence for typical values of D of 5×10^{-6} cm^{2} s^{-1} and of [E] of 10^{-6} M we find from (2) that

$$X_{\mathrm{k}} > 20\ \mu\mathrm{m}. \tag{4}$$

Using a ring-disc electrode, we have shown that [M] $< 10^{-7}$ M. Substitution in (3) gives

$$j < 2 \times 10^{-13}\ \mathrm{mol\ cm^{-2}\ s^{-1}}.$$

This result may be compared with observed values of j, which are about 3×10^{-9} mol cm^{-2} s^{-1}. The organic salt is too insoluble, and the homogeneous kinetics too sluggish, to explain the observed flux.

Furthermore, from figure 5 it can be seen that one of the features of our $TTF^{+}TCNQ^{-}$ electrodes is their large surface area and roughness. P.N.B. has grown single-crystal electrodes; a comparison of the fluxes observed on the single crystal and on the porous electrodes suggests a roughness factor of between 10^{2} and 10^{3}. The spacing between the crystallites in figure 5 is 10 μm or less, but in (4) we estimate that the reaction layer thickness would have to be more than 20 μm. Such a thick reaction layer would mean that the layer from one crystalite would overlap that of its nearest neighbours. There would be little advantage in having the porous electrode compared to the single crystal; the roughness factor would be close to unity rather than having the observed value, which is greater than 100. Finally, when one inserts dialysis membrane between the enzyme and the electrode, no activity is observed. For all these reasons we conclude that the reaction does not take place by homogeneous mediation but that the enzyme does react on the surface of the electrode.

PHILOSOPHICAL TRANSACTIONS OF THE ROYAL SOCIETY B BIOLOGICAL SCIENCES

FIGURE 5. Scanning electron micrograph of the surface of a $TTF^{+}TCNQ^{-}$ electrode. The strands of polymer binder can be seen.

Results for the variation of the rate of oxidation of glucose oxidase with electrode potential are displayed in figure 6. Unlike NADH, the reaction rate does depend on potential, although the value of the transfer coefficient, α, of about 0.3 is lower than normal. For the single-crystal electrode, results for the variation of the reaction rate with enzyme concentration are plotted in figure 7. We find the order with respect to [E] is one half rather than unity. This result is consistent with (3) above, but is not consistent with a mechanism in which there is a direct electron transfer from the enzyme to the electrode.

We therefore propose that the reaction of the enzyme on the conducting organic salt electrode takes place by heterogeneous redox catalysis as opposed to direct electron transfer. The simplest form of such a mechanism is as follows:

$$TTF^{+}TCNQ^{-} \overset{K_1}{\rightleftharpoons} TTF^{0} + TCNQ^{0}$$

$$TTF^{0} \xrightarrow{k_2,\ j} TTF^{+} \qquad TCNQ^{0} \xrightarrow{k_3[E],\ j} TCNQ^{-}$$

In this mechanism TTF^{0} and $TCNQ^{0}$ are species adsorbed on the surface; to obtain second-order kinetics, one of the species has to be mobile on the surface.

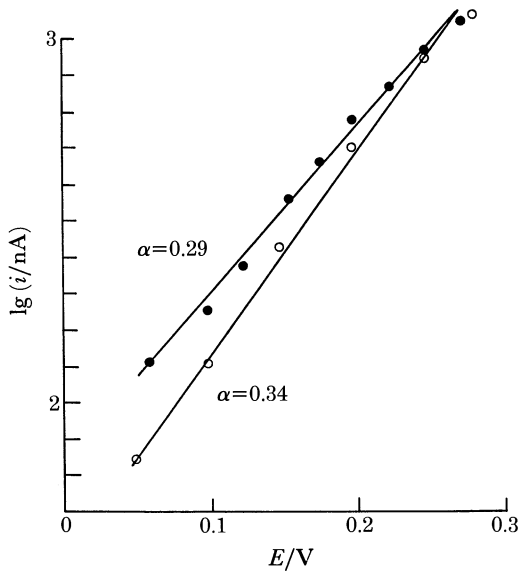

FIGURE 6. Typical Tafel plots for the oxidation of glucose oxidase on a $TTF^{+}TCNQ^{-}$ electrode (E measured against an SCE).

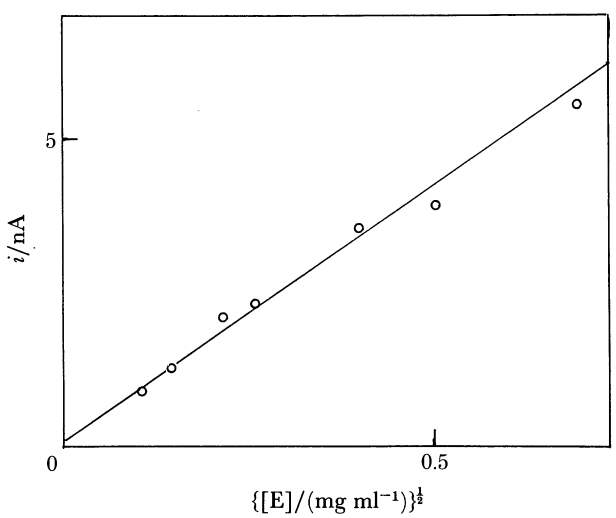

FIGURE 7. Results for the glucose oxidase system, showing that the current depends on $[E]^{\frac{1}{2}}$.

Steady-state analysis of this mechanism gives the following results:

$$[TTF^{0}][TCNQ^{0}] = K_1,$$

and

$$j = k_2[TTF^{0}] = k_3[TCNQ^{0}][E] = \sqrt{(K_1 k_2 k_3[E])}. \qquad (5)$$

In agreement with experiment, the reaction order with respect to [E] is $\frac{1}{2}$. Furthermore if either k_2 or k_3 has a normal value of the transfer coefficient, α, of 0.5, then the square root in (5) means that the observed value of α will be about 0.25. The three different mechanisms and the experimental results are compared in table 3.

TABLE 3. COMPARISON OF THE THREE MECHANISMS

	homogeneous mediation	direct transfer	heterogeneous redox catalysis	experimental results
order w.r.t. E	$\frac{1}{2}$	1	$\frac{1}{2}$	$\frac{1}{2}$
α	0, $\frac{1}{2}$, or 1	$\frac{1}{2}$	$\frac{1}{4}$	$\frac{1}{4}$
ring-disc	yes	no	no	no
roughness factor	no	yes	yes	yes

IN VIVO MEASUREMENT OF GLUCOSE

In collaboration with Dr M. Fillenz and Mr M. G. Boutelle, of the Department of Physiology, University of Oxford, we have been able to make microelectrodes of $TTF^{+}TCNQ^{-}$ for monitoring glucose in the brain of a freely moving rat. After soaking the electrode in a solution of glucose oxidase for several hours, we find that the enzyme is so strongly adsorbed that it cannot be removed by repeated washing or soaking in buffer solutions. In figure 8 we display typical calibration curves for the microelectrodes. It can be seen that there is negligible loss of activity over a period of 10 h implantation. Even after 28 d the electrode is still reasonably active. In figure 9 we show a comparison of the response of an implanted electrode to an injection of insulin with results obtained simultaneously by Dr Claire Stanford using blood samples and a conventional Yellow Springs glucose analyser. Excellent agreement is found. These results are most encouraging for the use of *in vivo* enzyme electrodes; the development of such electrode is not only important for clinical practice but will also be an important technique throughout animal and plant physiology.

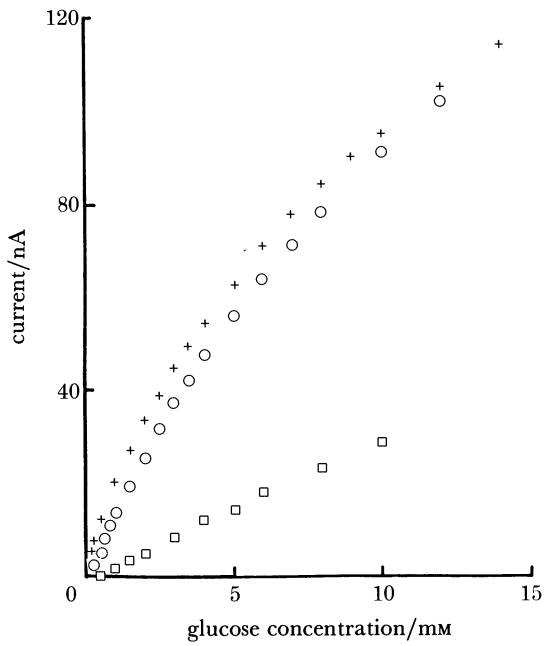

FIGURE 8. Calibration plots for *in vivo* glucose electrodes: +, before implantation; ○, after 10 h implantation; □, after 28 days implantation.

PHILOSOPHICAL TRANSACTIONS OF THE ROYAL SOCIETY B BIOLOGICAL SCIENCES

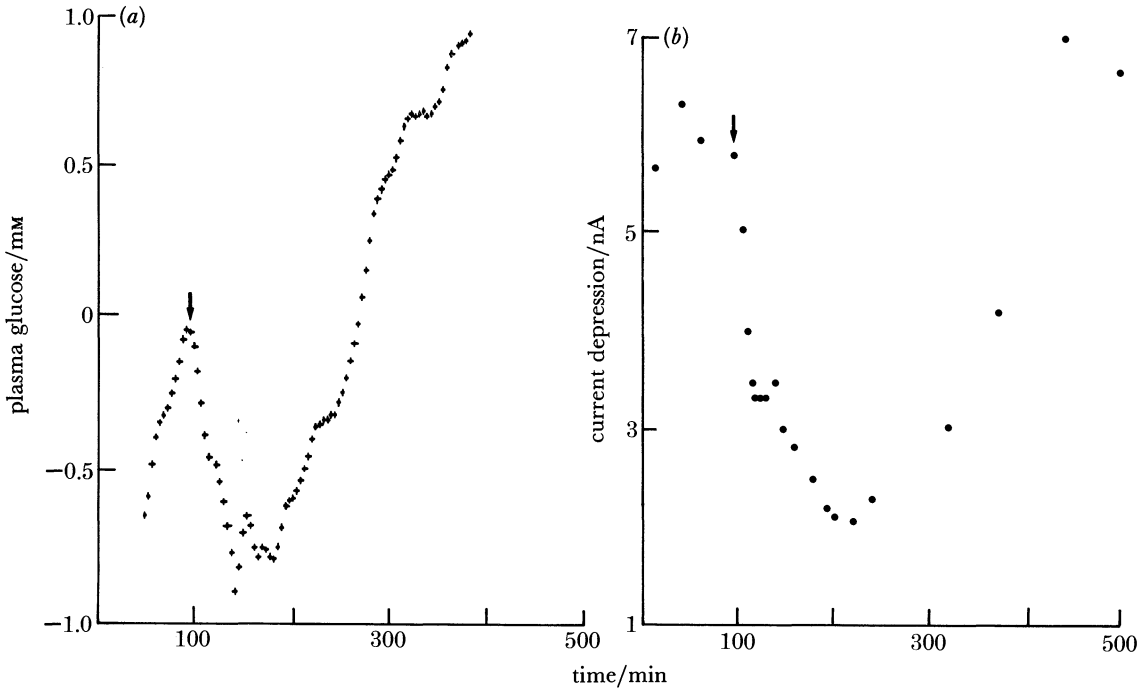

FIGURE 9. Comparison of the response from an implanted glucose electrode (*a*) with blood glucose as determined from blood samples (*b*) to an injection of insulin (25 units kg^{-1}).

THE CHEMICAL CANARY

Our final example is a sensor for low levels of toxic gases, such as H_2S or HCN. The levels are too low for the current from the direct reduction or oxidation of the gas molecules to be measurable; instead, we construct a chemical canary in which the respiratory enzyme cytochrome oxidase does its normal job of reducing oxygen. The rate of this reaction is

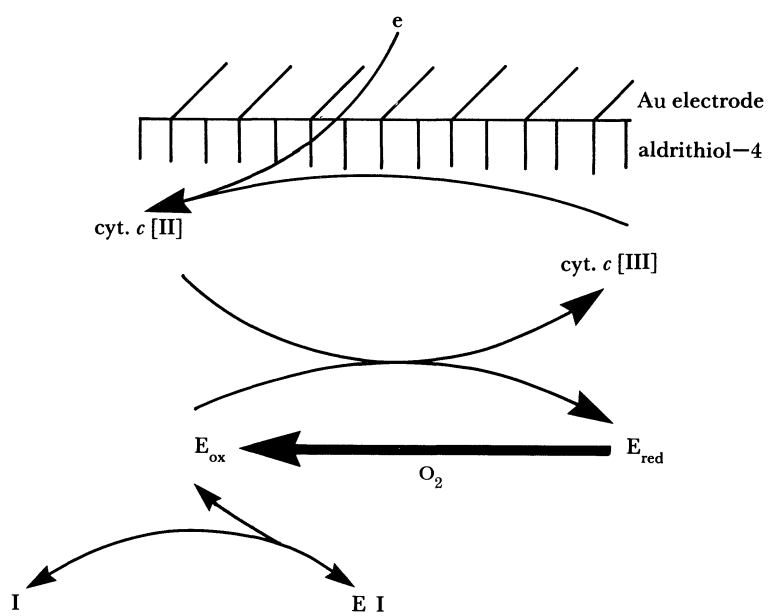

FIGURE 10. The chemical canary. The enzyme, E, is cytochrome oxidase.

PHILOSOPHICAL TRANSACTIONS OF THE ROYAL SOCIETY B BIOLOGICAL SCIENCES

monitored through the coupled reactions of cytochrome *c* and a modified gold electrode (figure 10). On arrival of the toxic inhibitor I, the enzyme, E, is removed as the complex EI, and the current falls. Typical results are shown in figure 11. We have shown that the rate of this process is controlled by the relaxation kinetics of the E–EI equilibrium:

$$\mathrm{E}+\mathrm{I} \underset{k_{-2}}{\overset{k_2}{\rightleftharpoons}} \mathrm{EI},$$

with

$$\ln\left[(i_t-i_\infty)/(i_0-i_\infty)\right] = -\{k_2[\mathrm{I}]+k_{-2}\}t. \tag{6}$$

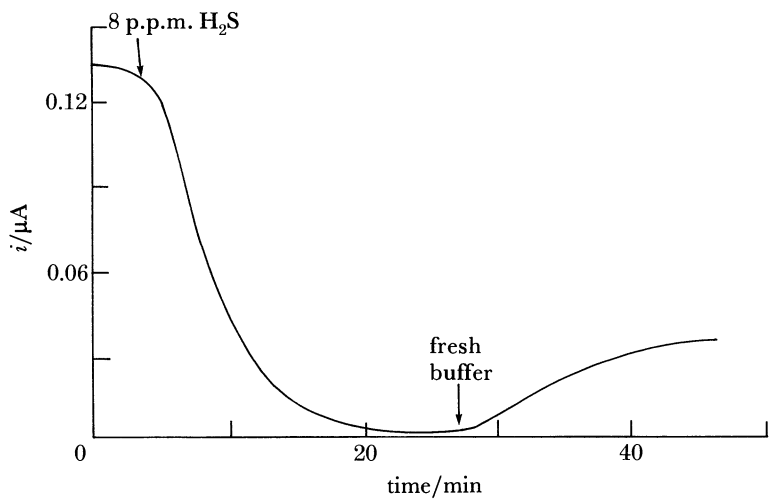

FIGURE 11. Typical current–time trace showing the inhibition of the enzyme on the admission of H_2S.

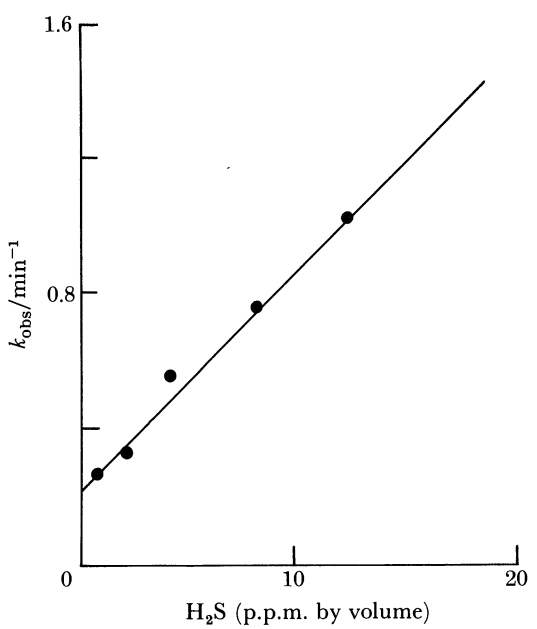

FIGURE 12. Results for the observed first-order rate constant, k_{obs}, plotted against $[H_2S]$ according to equation (6).

PHILOSOPHICAL TRANSACTIONS OF THE ROYAL SOCIETY B BIOLOGICAL SCIENCES

The results in figure 11 show that the observed rate constants do indeed obey (6); the ratio of the rate constants is in reasonable agreement with published values for the inhibition constant for EI (Nicholls 1975). It can be seen that concentrations as low as 2 parts per million (by volume) can be measured using this technique. These very low levels can be measured because each molecule of H_2S 'kills' a molecule of active enzyme catalyst. The isolation of vital molecular biochemistry in this way, and its direct transduction into current, should lead to the development of a range of sensors for monitoring the environment.

We thank our collaborators for their contributions to the work reported in this paper: NADH electrodes, Dr B. Lennox and Dr K. W. Sim; organic-salt electrodes, Dr C. P. Wilde, Dr D. H. Craston, B. J. Driscoll and L. Murphy; *in vivo* glucose electrodes, Dr M. Fillenz and M. G. Boutelle; the chemical canary, Dr Z. X. Shu. Financial assistance is also gratefully acknowledged from the S.E.R.C., the M.R.C., B.P., G.E.C. and Genetics International.

References

Albery, W. J. & Bartlett, P. N. 1984 An organic conductor electrode for the oxidation of NADH. *J. chem. Soc. chem. Commun.* 234–236.

Albery, W. J. & Bartlett, P. N. 1985 Amperometric enzyme electrodes – part 1: theory. *J. electroanalyt. Chem.* **194**, 211–222.

Albery, W. J., Bartlett, P. N. & Craston, D. H. 1985 Amperometric enzyme electrodes. 2. Conducting salts as electrode materials for the oxidation of glucose oxidase. *J. electroanalyt. Chem.* **194**, 223–245.

Albery, W. J., Bartlett, P. N., Bycroft, M., Craston, D. H. & Driscoll, B. J. 1987 Amperometric enzyme electrodes. 3. A conducting salt electrode for the oxidation of four different flavoenzymes. *J. electroanalyt. Chem.* **218**, 119–126.

Berman, T. E. 1969 *Enzyme handbook*, vol. 2, p. 23. New York: Springer-Verlag.

Boutelle, M. G., Stanford, C., Fillenz, M., Albery, W. J. & Bartlett, P. N. 1987 An amperometric enzyme electrode for continuous monitoring of brain glucose in the freely moving rat. *Neurosci. Lett.* **72**, 283–288.

Burstein, C., Ounissi, H., Legoy, M. D., Gellf, G. & Thomas, D. 1981 Recycling of NAD^+ using co-immobilised alcohol dehydrogenase and *E. coli*. *Appl. Biochem. Biotechnol.* **6**, 329–338.

Cenas, N. K. & Kulys, J. J. 1981 Biocatalytic oxidation of glucose on the conductive charge transfer complexes. *Bioelectrochem. Bioenergetics* **8**, 103–113.

Koutecky, J. & Levich, V. G. 1956 The use of a rotating disc electrode for studying kinetic and catalytic processes in electrochemistry. *Russ. J. phys. Chem.* **32**, 1565–1570.

Kulys, J. J., Samalius, A. S. & Svirmickas, G. J. S. 1980 Electron exchange between the enzyme active centre and organic metal. *FEBS Lett.* **114**, 7–10.

Kulys, J. J., Cenas, N. K., Svirmickas, G. J. S. & Svirmickiene, V. P. 1982 Chronoamperometric stripping analysis following biocatalytic preconcentration. *Analytica chim. Acta* **138**, 19–26.

Kulys, J. J. & Samalius, A. S. 1983 Kinetics of biocatalytic current generation. *Bioelectrochem. Bioenergetics* **10**, 385–393.

Nicholls, P. 1975 The effect of sulphide on cytochrome aa_3 – isosteric and allosteric shifts of the reduced α-peak. *Biochim. Biophys. Acta* **396**, 24–35.

Discussion

R. Eisenthal (*Biochemistry Department, University of Bath, U.K.*). 1. As the ideal biosensor is 'reagentless', one of the difficulties in developing biosensors based on NAD(P)-dependent dehydrogenases must involve immobilizing the pyridine nucleotide cofactor. What methods has Professor Albery considered for surmounting the problem of the soluble cofactor? One approach might be to bind the coenzyme covalently to the enzyme, thus converting the coenzyme into a prosthetic group, and making possible what would be, in effect, a third-generation biosensor.

2. In Professor Albery's description of the ethanol biosensor based on ethanol dehydrogenase,

the response of the sensor to ethanol concentration was governed by the kinetics of the enzyme. One possibility of overcoming limitations that this might impose would be to alter the kinetic constants of the reaction by using NAD analogues such as those developed by Kaplan in the 1950s.

W. J. Albery. I quite agree that it is desirable to trap the NAD^+ behind the membrane. We are pursuing two strategies to achieve that end. First we have shown that the sensor works with NAD^+ attached to a dextran where the dialysis membrane retains the modified NAD^+. The enzyme kinetics are somewhat slower, so there is some loss in sensitivity. Our second strategy is to design a membrane that will retain NAD^+/NADH but allow passage of the substrate and product. Because both NAD^+ and NADH are negatively charged, a permselective membrane with anionic charge may be able to achieve the necessary selectivity. We are investigating this approach at Imperial College in collaboration with Dr Barrie and Dr George.

As regards the second suggestion, we are not too unhapy with the enzyme kinetics as they are at present.

I. J. Higgins (*Biotechnology Centre, Cranfield Institute of Technology, Bedford, U.K.* and *The Leicester Biocentre, Leicester University, U.K.*). Dr Turner, Dr Cardosi and Mr Hendry from Cranfield have recently shown that both donor and acceptor components of conducting salts (e.g. TTF and TCNQ), adsorbed to graphite by similar procedures to those used to make ferrocene electrodes, function extremely well as biosensors when redox enzymes such as glucose oxidase are immobilized on the carbon surface. Does Professor Albery feel that these findings are consistent with his current views of the mechanism of electron transfer from oxidases to conducting salts?

W. J. Albery. I believe that the finding that the individual components of the conducting organic salt can catalyse the redox reaction of an enzyme adsorbed on graphite is consistent with the mechanism of heterogeneous redox catalysis proposed in our paper.

PHILOSOPHICAL TRANSACTIONS OF THE ROYAL SOCIETY B BIOLOGICAL SCIENCES

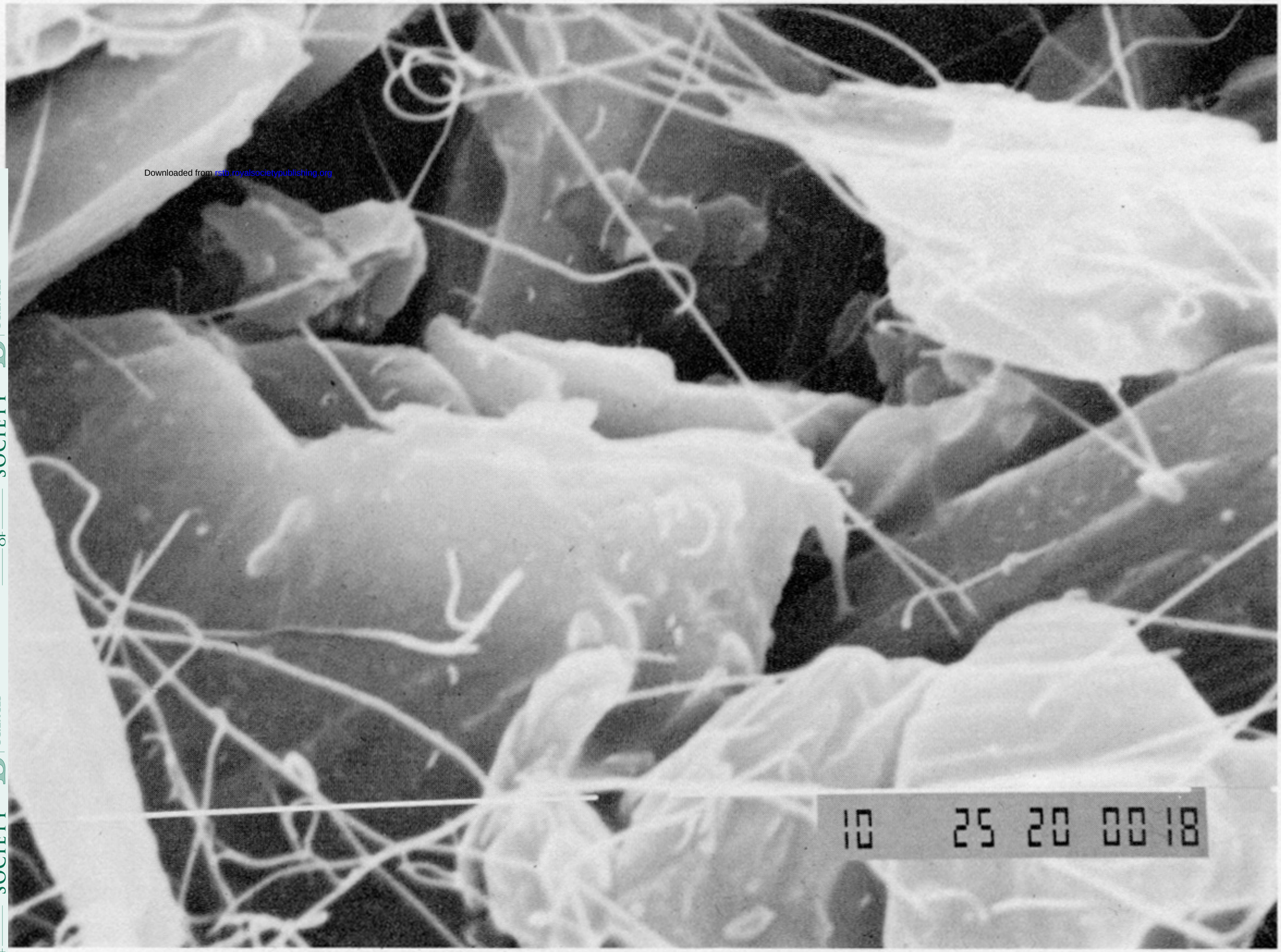

FIGURE 5. Scanning electron micrograph of the surface of a $TTF^{+}TCNQ^{-}$ electrode. The strands of polymer binder can be seen.

PHILOSOPHICAL TRANSACTIONS OF THE ROYAL SOCIETY B BIOLOGICAL SCIENCES